MOLECULAR ECOLOGY

**Supplementary information for:**

# Complexities of gene expression patterns in natural populations of an extremophile fish (*Poecilia mexicana*, Poeciliidae)

Courtney N. Passow, Anthony P. Brown, Lenin Arias-Rodriquez, M.-C. Yee, Alexandra Adams, Manfred Schartl, Wesley C. Warren, Carlos Bustamante, Joanna L. Kelley and Michael Tobler

**Table of Contents**

# Supplementary tables

**Table S1:** Collection localities of samples used in this study. For each site, we provided GPS coordinates, average standard length (mm) and mass (g) (± standard deviation) of females used.

| Site | Coordinates | Standard length (mm) | Mass (g) |
|---|---|---|---|
| Nonsulfidic surface (Arroyo Bonita) | 17.427, −92.752 | 45.25 ± 5.50 | 1.93 ± 0.50 |
| Sulfidic surface (El Azufre II) | 17.439, −92.775 | 32.75 ± 0.96 | 0.92 ± 0.11 |
| Nonsulfidic cave (Cueva Luna Azufre) | 17.441, −92.773 | 39.00 ± 5.35 | 1.71 ± 0.64 |
| Sulfidic cave (Cueva del Azufre) | 17.442, −92.775 | 43.25 ± 4.27 | 1.97 ± 0.37 |

**Table S2:** Descriptive statistics of RNA-sequencing reads for each population and organ before and after trimming. All numbers represent means (± standard deviation). Note, eye was not included due to low read mapping.

| Samples | Final sample size | Average raw read counts | Average read counts first trim | Average read counts second trim |
|---|---|---|---|---|
| Nonsulfidic surface, gill | 4 | 51,211,008 ± 3,066,659 | 50,494,010 ± 3,062,933 | 46,236,760 ± 2,694,877 |
| Nonsulfidic surface, liver | 4 | 43,796,910 ± 1,468,678 | 40,962,508 ± 1,096,851 | 37,645,326 ± 1,019,676 |
| Nonsulfidic surface, brain | 4 | 36,697,772 ± 3,592,346 | 35,880,998 ± 3,458,547 | 32,552,250 ± 2,950,330 |
| Sulfidic surface, gill | 3 | 29,414,736 ± 3,279,715 | 28,104,778 ± 3,172,097 | 25,884,956 ± 3,027,642 |
| Sulfidic surface, liver | 4 | 42,558,146 ± 4,628,663 | 41,840,232 ± 4,532,005 | 37,832,356 ± 3,769,800 |
| Sulfidic surface, brain | 2 | 15,295,696 ± 142,168 | 14,998,258 ± 135,061 | 13,544,718 ± 318,171 |
| Nonsulfidic cave, gill | 3 | 29,879,398 ± 947,819 | 29,344,370 ± 892,075 | 26,783,182 ± 487,324 |
| Nonsulfidic cave, liver | 4 | 33,927,432 ± 2,481,755 | 31,915,320 ± 2,427,735 | 29,008,504 ± 2,190,784 |
| Nonsulfidic cave, brain | 2 | 19,994,198 ± 5,192,999 | 18,891,230 ± 4,895,510 | 17,487,216 ± 4,497,547 |
| Sulfidic cave, gill | 4 | 39,945,364 ± 3,928,399 | 38,620,432 ± 3,981,537 | 34,880,386 ± 3,299,396 |
| Sulfidic cave, liver | 4 | 38,152,448 ± 2,765,622 | 35,404,608 ± 1,955,737 | 32,293,256 ± 1,633,588 |
| Sulfidic cave, brain | 3 | 35,553,494 ± 5,145,134 | 34,852,068 ± 5,095,666 | 31,790,312 ± 4,734,325 |

**Table S3:** Descriptive statistics for the alignment to the *Poecilia mexicana* genome and assembly of the reference transcriptome. Most metrics were determined from the perl script assemblathon_stats.pl written by Keith Bradnam (UC Davis) and licensed under a Creative Commons Attribution-NonCommercial-ShareAlike 3.0 Unported License.

| Metric | Value |
|---|---|
| Total number of unique transcripts | 63,590 |
| Total number of unique loci | 38,764 |
| Mean contig size | 3,568 |
| Median contig size | 2,796 |
| N50 (base pairs) | 5,290 |
| Longest contig | 103,334 |
| Total number of bases in transcriptome | 225,876,000 |
| GC % | 46.82% |

**Table S4:** Annotation results of the 48,242 transcripts with hits in the human SwissProt database. For each transcript (specified by TCONS number), the table includes information on the sequence ID from SwissProt (including the accession number), percent of similarity, alignment length, number of mismatches, number of gap openings, start and end of the alignment query, start and end of the alignment subject, E-value, and the bit score of the top BLAST hit for each transcript. Due to the large size, the table is provided in a separate Excel spreadsheet ("Table S4 – Reference Annotations.xlsx")

**Table S5:** Results of the enrichment analysis of Gene Ontology (GO) terms of differentially expressed transcripts that were unique to each organ analyzed. Provided are the GO term identification number, description of the enriched GO term, the total number of genes in each reference set (N), the total number of genes with a specific GO term in each reference (B), the number of genes in the target set (n), and the number of genes in the intersections (b), *P*-value associated with the enrichment, false-discovery rate (*q*-value), and enrichment value obtained from Gorilla enrichment analysis. Due to the large size, the table is provided in a separate Excel spreadsheet ("Table S5 – Unique GO annotations.xlsx"). Each tab corresponds to the unique enriched GO terms for each organ. Enriched GO terms associated with upregulated transcripts are colored blue whereas enriched GO terms associated with downregulated transcripts are colored red.

**Table S6:** Results of the enrichment analysis of Gene Ontology (GO) terms of differentially transcripts that were shared between environments (sulfidic and cave) for each of the organs (gill, liver and brain). Provided are the GO term identification numbers, description of the enriched GO term, and gene names within each GO category obtained from the GOrilla enrichment analysis. We report the GO terms for differentially expressed genes that were (A) upregulated in the sulfur populations, (B) downregulated in the sulfur populations, (C) upregulated in the cave environments, and (D) downregulated in the cave environments. Note, that we only report shared responses with terms associated with biological processes.

| GO ID | Description | Gene names |
|---|---|---|
| **A. Sulfur upregulated** | | |
| *Gill* | | |
| GO:0044272 | Sulfur compound biosynthetic process | MLYCD, ACOT13, ACSS2, ACOT4, GSTM3, GSS, CDO1, ELOVL4, SLC25A1, GCLM, CHAC2, OGN, GSTZ1, ELOVL7, GCLC, MPST, MGST1, NCAN, ACSL1, SLC26A2, B3GNT7, GGT1, AKR1A1, MPC1, GSTO1, ELOVL6, CHAC1, GGT5 |
| GO:0019752 | Carboxylic acid metabolic process | PRKAG2, PRKAB1, TPI1, IL4I1, GADL1, SLC7A8, CNDP2, PSAT1, PGD, LPIN1, GLO1, BAAT, FABP6, ABCB11, CYP2J2, GSS, CDO1, IVD, SQRDL, PDK3, GSTZ1, GCLC, ELOVL7, RGN, PCK1, HNMT, ELOVL5, ABHD10, P4HB, GGH, PTGR1, SLC1A3, PLA2G10, ETHE1, PFKL, SRD5A2, SLC22A4, CCBL2, FADS2, CKB, MPST, NCAN, CRAT, SLC25A10, IDNK, HSD17B8, MLYCD, PGK1, PRKAB1, GADL1, PSAT1, PGD, ABCB11, GSS, MCEE, GCSH, GSTZ1, ELOVL7, ACADL, ACADS, ABHD10, GGH, P4HA1, PADI2, PARS2 |
| GO:0016051 | Carbohydrate biosynthetic process | PGK1, PCK2, PRKACB, PCK1, TPI1, AKR1B1, PGD, SLC25A1, PPP1R3C, GYS1, TALDO1, SLC25A10, G6PD, NR1D1, B3GNT3, B3GNT2, FBP1, RGN |
| GO:0044281 | Small molecule metabolic process | ACOT13, GADL1, GSTM3, GSR, COX5B, HSD11B1, APOB, APOA4, GSS, LPCAT4, COX15, GSTZ1, ELOVL7, SLC16A9, LIPH, CYCS, CERS6, CD36, NT5C2, P4HB, B3GNT3, GGH, CA5B, PTGR1, ECSIT, TTPA, GMPR2, CRAT, AQP1, CMBL, PRKAG2, TPI1, ADCK3, GLO1, CYP2J2, CDO1, CA4, SQRDL, CA2, PDK3, MAN2B2, GCLC, PCK2, PCK1, SLC25A1, SLC22A4, FBP1, MGST1, IDNK, MTTP, PRKAB1, SLC9A1, FABP2, SLC7A8, CNDP2, PSAT1, PGD, FABP6, ABCB11, PNP, CHIT1, ABCB1, LDLRAP1, UPP1, RGN, ELOVL5, ABHD10, SLC1A3, PLA2G10, ETHE1, ALDH3B1, PFKL, SLC4A1, RDH11, PCSK9, SLC2A4, ALAS2, CFTR, SLC5A1, G6PD, ACER1, IL4I1, AKR1B1, B3GNT2, LPIN1, BAAT, IVD, TXN, HNMT, ERVK-6, UCP2, SRD5A2, CCBL2, CHAC2, MPP1, CKB, HMOX2, MPST, NCAN, SLC25A10, GLTPD1, COX6B1, COX4I1, GCSH, PC, ACADL, ACADS, P4HA1, PADI2, GYS1, OGN, COQ6, BLVRB, FGF7, GCLM, MMADHC, TALDO1, SMS, ACOT4, ACSS2, FTCD, PPAP2B, KEAP1, PARS2, PDSS2, HSD17B8, MLYCD, PGK1, PRKACB, RFK, MCEE, SURF1, CHIA, PYGM, ELOVL4, PPP1R3C, |

| | | |
|---|---|---|
| | | AKR1B10, GPX1, NARS2, ABHD14B, GBAS, RDH14, HS3ST3A1, CYP26C1 |
| GO:1901700 | Response to oxygen-containing compound | TIE1, PRKACB, CAPN2, GSR, SLC8A1, APLP1, SLC14A2, CXCL12, GSS, GCNT1, SPARC, IRG1, WT1, MMP2, CYCS, CD38, GGH, CLDN4, GJA3, GJB2, WNT5A, NLRP1, PYGM, TRIM16, FKBP1B, PRDX1, SLC2A4, PCSK9, PDXP, CXCL6, G6PD, CFTR, AQP1, NR1D1, PPARGC1B, AKR1B1, CMA1, ABCC2, LITAF, GPX1, PDGFRB, PLAU, CDO1, RARG, WFDC1, SLC26A5, PDK3, GRN, PPBP, TXN, DMTN, TGFB3, PCK1, TSPO, SORT1, UCP2, TGFBR2, KLF4, YES1, CXCL2, RAMP3, CCRN4L, THBD, SPON2, MGST1, GJD3, BNIP3, PRDX6, SLC9A1, APOB, APOA4, SLC26A3, P2RY6, CD36, P4HB, PFKL, KLF15, LPIN1, SLC22A6, MDM2, LYN, KRT8, EIF2AK2, HNMT, CDKN1A, HAVCR2, SRD5A2, ILDR2, IRF5 |
| GO:0044283 | Small molecule biosynthetic process | PRKAG2, PHOSPHO1, PRKAB1, ACER1, TPI1, GADL1, ADCK3, AKR1B1, LPIN1, PSAT1, PGD, BAAT, ABCB11, APOA4, CDO1, PNP, ELOVL7, RGN, PCK2, PCK1, ELOVL5, SLC1A3, SLC25A1, FADS2, FBP1, NCAN, SLC25A10, CFTR, G6PD, HSD17B8, PDSS2, MLYCD, PRKACB, RFK, FGF7, PC, TALDO1, ACSS2, PADI2, ELOVL4, COQ6 |
| GO:1901564 | Organonitrogen compound metabolic process | MLYCD, GLTPD1, PGK1, GADL1, GSTM3, RFK, GSR, PSAT1, PGD, GSS, LPCAT4, MCEE, MRPS18A, SURF1, GCSH, PC, COX15, GSTZ1, ACADL, TUFM, NT5C2, CTSZ, P4HA1, GGH, CHIA, SLC1A3, PADI2, PLA2G10, ETHE1, GMPR2, ALDH3B1, PFKL, ABCB6, PPP2CA, OGN, BLVRB, ALAS2, PDXP, CRAT, G6PD, AQP1, SLC25A35, MRPS16, ACER1, TPI1, IL4I1, AKR1B1, CMA1, PDGFRB, GPX1, NARS2, GLO1, FGF7, CDO1, IVD, SQRDL, GCLM, MRPS15, MMADHC, TALDO1, SLC25A51, ABHD14B, MRPL38, GCLC, SMS, GBAS, TSFM, TSPO, MRPL15, FTCD, HS3ST3A1, MRPS17, UCP2, SLC25A1, CCBL2, SCG5, CHAC2, PPAP2B, CKB, HMOX2, MPST, NCAN, SLC25A10, PARS2, MGST1, SLC7A8, SLC9A1, CNDP2, APOA4, PNP, CHIT1, SLC16A9, UPP1, CERS6, B3GNT3, P4HB, GFM1, NACA, PRKAG2, SLC25A38, PHOSPHO1, LPIN1, B3GNT2, BAAT, AMBP, ITIH3, EIF2AK2, HNMT, ERVK-6, SLC22A4, MPP1, ANPEP |
| GO:0009725 | Response to hormone | PPARGC1B, GSTM3, AKR1B1, ABCC2, SLC9A1, LPIN1, CXCL12, APOB, MDM2, CDO1, CA2, SLC26A5, LYN, GRN, GCLC, TRIM25, CTSL, SLC34A2, HNMT, PCK1, P2RY6, GGH, CLDN4, CDKN1A, GJB2, UCP2, TGFBR2, RAMP3, ANXA2, SRD5A2, TRIM16, PCSK9, SLC2A4, LMO2, AQP1, PAQR8, NR1D1, PRKACB, PDGFRB, GCNT1, WFDC1, SPARC, ACADS, IRG1, WT1, LOX, S100B, CD38, TGFB3, TSPO, SORT1, MMP14, WNT5A, PAQR6, SMAD6, KEAP1 |
| GO:0042592 | Homeostatic process | PRKACB, GSR, SFXN5, FBXW7, SLC35G1, SLC8A1, CXCL12, TRPC4, ARRDC3, UMOD, TRPM2, SLC9A2, FTH1, ACADL, LDLRAP1, ACADS, FOXO3, PARP3, ATP6V1E1, CTSK, CD38, CXCR3, CLDN4, PLA2G10, GRHL3, PYGM, ABCB6, SLC4A1, FKBP1B, SLC26A11, |

| | | |
|---|---|---|
| | | PRDX1, PCSK9, SLC2A4, ALAS2, RAC1, CFTR, AQP1, NR1D1, AKR1B1, CMA1, ABCC2, GPX1, FGF7, PLAU, TMEM79, IVD, SCO1, CA2, PDK3, SLC26A5, GCLC, TXN, CYBRD1, GRIK2, PCK1, FADD, UCP2, MAFG, TXNRD3, EPOR, ABCA12, CKB, HMOX2, NR1D2, TRPV4, CNGB1, ALOXE3, GPR116, FN1, SLC9A3R1, ATP2A2, CRY1, WNK4, IRS1, ATP1A1, STAT5B, FGF23, CCR1, ATP1B1, LDLR, FLVCR1, SLC9A3, ATM, SSTR5, ITPKB, KCNMA1, KRT16, CHP1, MUC2, ANG, NGFR, CCDC109B, ATP6AP1, INSR, RHCG, SLC9A6, SOX4, SLC22A5, KCNJ2, SLC26A2, ERP44, HFE, TNFSF11, ATP2B3, PIGR |
| GO:0015701 | Bicarbonate transport | CA4, SLC4A10, SLC4A1, CA2, SLC26A5, SLC26A11, SLC26A3, CA5B, CFTR, AQP1 |
| GO:0048878 | Chemical homeostasis | TRPV4, GPR116, ALOXE3, PVALB, MICU1, FN1, SLC9A3R1, ATP2A2, XPR1, CRY1, WNK4, IRS1, ATP1B1, LDLR, UMOD, TRPM2, KCNMA1, NGFR, ATP6AP1, INSR, ADCY9, CCL14, CLDN4, SLC39A6, KCNJ2, ATP6V1C1, PTPN11, SLC4A1, TRPV1, HFE, SLC25A23, RAB38, GPER1, ATP2B3, PTPRC, SLC4A10, CMA1, SLC7A8, ABCC2, SLC9A1, SLC35G1, CXCL12, APOB, APOA4, PLAU, TMEM79, TRPC4, IVD, CA2, SLC26A5, PDK3, SLC9A2, FTH1, SLC26A3, LDLRAP1, FOXO3, RGN, CYBRD1, ATP6V1E1, SLC34A2, PCK1, CD36, PLA2G10, UCP2, GRHL3, TTPA, MAFG, ABCA12, SLC31A1, FKBP1B, SLC26A11, SLC2A4, CLDN1, PCSK9, ALAS2, CKB, HMOX2, NR1D2, CFTR, AQP1 |
| GO:0046364 | Monosaccharide biosynthetic process | SLC25A1, PCK2, PCK1, TPI1, FBP1, AKR1B1, SLC25A10, PGD, G6PD, RGN, PGK1, PRKACB, PC, TALDO1 |
| GO:0055114 | Oxidation-reduction process | HSD17B8, PGK1, COX6B1, PRKACB, GSR, COX4I1, COX5B, PGD, MICAL1, BLOC1S2, MCEE, SURF1, COX15, FTH1, ACADL, ACADS, LOX, CYCS, ALKBH1, P4HA1, PIR, ETHE1, PYGM, GMPR2, ALDH3B1, PFKL, PPP1R3C, BMP2, GYS1, RDH11, AKR1B10, PRDX1, COQ6, BLVRB, CRAT, LEPREL1, PPP1R2, G6PD, NR1D1, PMPCB, TPI1, IL4I1, AKR1B1, GPX1, EPX, CDO1, IVD, PXDN, SQRDL, RFESD, TALDO1, SDHAF2, TXN, CYBRD1, SDR42E2, ACSS2, RDH14, SDR39U1, UCP2, CYP26C1, TXNRD3, RDH16, DUS3L, HMOX2, MTO1, SLC25A10, MGST1, DHRS13, PRKAG2, PRDX6, CYP2J2, HEPHL1, ALKBH3, PTGR1, ECSIT, PCDH12, SRD5A2, FADS2 |
| GO:0006749 | Glutathione metabolic process | CHAC2, GSTM3, GSR, GSTZ1, GCLC, CNDP2, G6PD, MGST1, GLO1, ETHE1, GSS, GCLM, GPX1 |
| GO:0042221 | Response to chemical | IL18, HAT1, GSTM3, GSR, COX4I1, APLP1, SLC14A2, CXCL12, CD274, GSS, GCNT1, SPARC, ACADS, FOXO3, IRG1, MMP2, LOX, CYCS, CD38, GGH, CLDN4, MMP14, GJA3, GJB2, BMP2, TRIM16, PRDX1, FKBP1B, LMO2, CXCL6, AQP1, NR1D1, PPARGC1B, LITAF, ABCC2, PDGFRB, CDO1, WFDC1, CA2, PDK3, GCLM, MEFV, PPBP, GCLC, CYBRD1, S100B, ADD3, PCK1, TSPO, SLC7A11, C1QA, SOX6, DNAJC4, SNAI2, RAMP3, |

| | | |
|---|---|---|
| | | PAQR6, KEAP1, MGST1, PAQR8, TIE1, PRKACB, CAPN2, SLC8A1, UMOD, WT1, CTSL, HLA-DPA1, SLC1A3, WNT5A, PYGM, NLRP1, ALDH3B1, PFKL, CLEC3B, PPP2CA, PCSK9, SLC2A4, PDXP, CFTR, G6PD, RALB, ACER1, CMA1, AKR1B1, TNMD, GPX1, RARG, PLAU, SLC26A5, NDRG1, GRN, CLU, RAP2A, TXN, TMEM100, DMTN, TGFB3, SERPINH1, SORT1, TRIM21, CHP2, UCP2, TGFBR2, KLF4, YES1, CXCL2, ANXA2, CCRN4L, FAM162A, THBD, SPON2, SMAD6, MPST, GJD3, GAS1, PRDX6, BNIP3, SLC7A8, SLC9A1, APOB, APOA4, XAF1, PNP, ABCB1, SLC26A3, TRIM25, CD36, P2RY6, P4HB, PTGR1, TTPA, KLF15, LPIN1, SLC22A6, MDM2, LYN, KRT8, EIF2AK2, SLC34A2, HNMT, CDKN1A, HAVCR2, SLC31A1, SRD5A2, ILDR2, IRF5, FBP1 |
| GO:0006790 | Sulfur compound metabolic process | MLYCD, ACOT13, GSTM3, GSR, GPX1, MICAL1, GLO1, GSS, MCEE, CDO1, SQRDL, GCLM, PC, ABHD14B, GSTZ1, GCLC, ELOVL7, TXN, SMS, ACOT4, ACSS2, ETHE1, ELOVL4, SLC25A1, CHAC2, OGN, MPST, NCAN, KEAP1, SLC25A10, MGST1, G6PD, ELOVL5, B3GNT3, CNDP2, B3GNT2, BAAT |
| GO:0006979 | Response to oxidative stress | PPARGC1B, PRDX6, BNIP3, GSR, AKR1B1, ABCC2, MDM2, GSS, APOA4, PXDN, SEPP1, GCLC, FOXO3, TXN, CYCS, SLC7A11, CD36, P4HB, GJA3, GJB2, UCP2, KLF4, ALDH3B1, FKBP1B, PRDX1, MGST1, G6PD, AQP1, GPX1, SLC8A1, PDGFRB, EPX, GCLM, TRPM2, CD38, MMP14 |
| GO:0009719 | Response to endogenous stimulus | PRKACB, CAPN2, GSTM3, SLC8A1, APLP1, CXCL12, GSS, GCNT1, SPARC, ACADS, IRG1, WT1, MMP2, LOX, CTSL, CD38, GGH, CLDN4, MMP14, GJB2, WNT5A, NLRP1, PYGM, CLEC3B, BMP2, TRIM16, SLC2A4, PCSK9, LMO2, PDXP, CFTR, AQP1, NR1D1, PPARGC1B, AKR1B1, ABCC2, PDGFRB, TNMD, PLAU, CDO1, WFDC1, CA2, SLC26A5, GRN, GCLC, DMTN, TMEM100, S100B, TGFB3, PCK1, TSPO, SORT1, SLC7A11, SOX6, UCP2, TGFBR2, KLF4, SNAI2, YES1, ANXA2, RAMP3, PAQR6, THBD, SMAD6, KEAP1, MGST1, PAQR8, SLC9A1, APOB, SLC26A3, TRIM25, CD36, P2RY6, KLF15, LPIN1, SLC22A6, MDM2, LYN, SLC34A2, HNMT, CDKN1A, SRD5A2, IRF5 |
| GO:0006575 | Cellular modified amino acid metabolic process | GSTM3, FTCD, GSR, P4HA1, GGH, GPX1, PLA2G10, PADI2, GLO1, ETHE1, GSS, LPCAT4, GCLM, CCBL2, CHAC2, CKB, GSTZ1, GCLC, MPST, MGST1, G6PD, P4HB, CNDP2 |
| GO:0010033 | Response to organic substance | IL18, CAPN2, GSTM3, SLC9A1, CXCL12, CD274, APOB, APOA4, GSS, XAF1, UMOD, SLC26A3, TRIM25, CTSL, P2RY6, CD36, GGH, CLDN4, GJB2, NLRP1, PFKL, CLEC3B, TRIM16, FKBP1B, SLC2A4, PCSK9, LMO2, G6PD, CFTR, AQP1, NR1D1, PPARGC1B, KLF15, AKR1B1, CMA1, LITAF, ABCC2, LPIN1, SLC22A6, MDM2, PLAU, CDO1, CA2, LYN, SLC26A5, PDK3, GRN, CLU, MEFV, GCLC, EIF2AK2, TMEM100, SLC34A2, PCK1, HNMT, SERPINH1, SLC7A11, CDKN1A, UCP2, TGFBR2, KLF4, HAVCR2, CXCL2, |

| | | |
|---|---|---|
| | | SRD5A2, RAMP3, ANXA2, ILDR2, CCRN4L, IRF5, MGST1, PAQR8, TIE1, PRKACB, SLC8A1, APLP1, GCNT1, SPARC, ACADS, IRG1, WT1, MMP2, LOX, CD38, HLA-DPA1, MMP14, WNT5A, PYGM, BMP2, PPP2CA, PDXP, CXCL6, RALB, TNMD, PDGFRB, RARG, WFDC1, PPBP, DMTN, S100B, TGFB3, TSPO, SORT1, TRIM21, SOX6, DNAJC4, SNAI2, YES1, PAQR6, THBD, SPON2, SMAD6, KEAP1, GAS1, GJD3 |
| *Liver* | | |
| N/A | N/A | N/A |
| *Brain* | | |
| GO:0006096 | Glycolytic process | GAPDH, LDHA, PGM1, GPI, PFKFB1, PFKM, ALDOA, PGAM2 |
| GO:0016051 | Carbohydrate biosynthetic process | PCK1, PGM1, B3GNT3, AKR1B1, AKR1A1, ALDOA, PGAM2, UBB, AGL, MPDU1, CHST8, GAPDH, GPI, GPD1, PFKFB1, NR1D1 |
| GO:0006757 | ATP generation from ADP | GAPDH, LDHA, PGM1, GPI, PFKFB1, PFKM, ALDOA, PGAM2 |
| **B. Sulfur downregulated** | | |
| *Gill* | | |
| GO:0055085 | Transmembrane transport | TRPV4, MAL, SLC6A6, ATP2A2, NDUFA4, SLC6A13, ATP1B1, AHCYL1, TRPM2, SLC25A15, SLC4A4, KCNMA1, SLC12A3, ATP6AP1, SLC5A7, SLC44A4, TRPM5, ATP6V1C1, SLC3A2, CYB561, TRPV1, SLC7A5, SLC4A1, SLC25A23, ATP2B3, SLC38A2, ATP8B1, PRKAG2, CNGB1, MICU1, PKD1L2, CALHM3, SLC25A25, SLC38A4, GABRD, SLC9B2, SLC25A22, SLC38A3, CLCN2, ADCY9, KCNJ15, SLC30A3, RTN2, SLC30A2, TRPM4, KCNJ2, SLC39A6, KCNJ1, SLC25A5, PTPRC, SLC25A12, SLC7A3, HSPA8, AFG3L2, PRF1, ATP1A1, SLC9A3, SLC9A2, FXYD1, CPT1A, CPT1B, CCDC109B, NIPAL4, RHCG, SLC9A6, SLC26A2, TSC22D3, ABCB10, FLVCR1, MPC1, SLC22A5, CLCN1, SLC22A4 |
| GO:0034220 | Ion transmembrane transport | PRKAG2, TRPV4, CNGB1, SLC6A6, ATP2A2, PKD1L2, NDUFA4, ATP1A1, ATP1B1, SLC38A4, TRPM2, SLC9A3, GABRD, SLC9A2, SLC4A4, MPC1, SLC25A22, KCNMA1, SLC12A3, SLC38A3, FXYD1, CLCN2, CPT1A, CPT1B, CCDC109B, ATP6AP1, KCNJ15, RHCG, SLC9A6, SLC22A5, KCNJ2, CLCN1, SLC3A2, SLC4A1, SLC26A2, SLC22A4, TSC22D3, ATP2B3, SLC25A12, ATP8B1, MICU1, CALHM3, SLC25A25, SLC9B2, SLC25A15, SLC30A3, SLC30A2, TRPM4, SLC39A6, TRPM5, ATP6V1C1, TRPV1, SLC7A5, KCNJ1, PTPRC, SLC7A3, SLC38A2 |
| GO:0030001 | Metal ion transport | TRPV4, CNGB1, MICU1, SLC9A3R1, ATP2A2, PKD1L2, WNK4, SLC25A25, ATP1B1, SLC38A4, TRPM2, SLC9B2, SLC4A4, KCNMA1, SLC12A3, SLC38A3, ATP6AP1, SLC5A7, KCNJ15, DNM2, SLC30A3, SLC30A2, TRPM4, SLC39A6, KCNJ2, ATP6V1C1, TRPM5, |

| | | |
|---|---|---|
| | | SLC3A2, TRPV1, HFE, KCNJ1, ATP2B3, PTPRC, SLC38A2, ATP1A1, CCR1, SLC9A3, SLC9A2, CHP1, CCDC109B, NIPAL4, SLC9A6, SLC22A5, SLC22A4 |
| GO:0006812 | Cation transport | PRKAG2, TRPV4, CNGB1, SLC9A3R1, ATP2A2, PKD1L2, WNK4, NDUFA4, ATP1A1, CCR1, ATP1B1, SLC38A4, TRPM2, SLC9A3, SLC9A2, SLC4A4, KCNMA1, SLC12A3, CHP1, SLC38A3, CPT1A, CPT1B, CCDC109B, ATP6AP1, SLC5A7, KCNJ15, NIPAL4, RHCG, SLC9A6, SLC22A5, KCNJ2, SLC44A4, SLC3A2, SLC22A4, HFE, ATP2B3, MICU1, SEC14L1, CALHM3, SLC25A25, SLC9B2, SLC25A15, DNM2, SLC30A3, SLC30A2, TRPM4, SLC39A6, TRPM5, ATP6V1C1, TRPV1, KCNJ1, PTPRC, SLC7A3, SLC38A2 |
| GO:0098655 | Cation transmembrane transport | PRKAG2, TRPV4, CNGB1, MICU1, ATP2A2, PKD1L2, CALHM3, NDUFA4, SLC25A25, ATP1B1, TRPM2, SLC9B2, SLC25A15, SLC4A4, KCNMA1, SLC12A3, SLC38A3, ATP6AP1, KCNJ15, SLC30A3, SLC30A2, TRPM4, SLC39A6, KCNJ2, TRPM5, ATP6V1C1, SLC3A2, TRPV1, KCNJ1, ATP2B3, PTPRC, SLC7A3, ATP1A1, SLC9A3, SLC9A2, CPT1A, CPT1B, CCDC109B, RHCG, SLC9A6, SLC22A5, SLC22A4 |
| GO:0006814 | Sodium ion transport | PRKAG2, TRPV4, CNGB1, ATP2A2, PKD1L2, NDUFA4, ATP1A1, ATP1B1, SLC9A3, TRPM2, SLC9A2, SLC4A4, KCNMA1, SLC12A3, SLC38A3, CPT1A, CPT1B, ATP6AP1, CCDC109B, KCNJ15, RHCG, SLC9A6, SLC22A5, KCNJ2, SLC3A2, SLC22A4, ATP2B3, MICU1, CALHM3, SLC25A25, SLC9B2, SLC25A15, SLC30A3, SLC30A2, TRPM4, SLC39A6, TRPM5, ATP6V1C1, TRPV1, KCNJ1, PTPRC, SLC7A3 |
| GO:0006811 | Ion transport | TRPV4, SEC14L1, SLC6A6, ATP2A2, WNK4, NDUFA4, SLC6A13, ATP1B1, LDLR, TRPM2, SLC25A15, SLC4A4, KCNMA1, SLC12A3, ATP6AP1, SLC5A7, SLC44A4, TRPM5, ATP6V1C1, SLC3A2, TRPV1, SLC7A5, SLC4A1, HFE, ATP2B3, SLC38A2, ATP8B1, PRKAG2, ATP8B4, CNGB1, MICU1, SLC9A3R1, PKD1L2, CALHM3, SLC25A25, SLC38A4, GABRD, SLC9B2, SLC25A22, SLC38A3, CLCN2, KCNJ15, DNM2, SLC30A3, SLC30A2, PITPNC1, TRPM4, SLC39A6, KCNJ2, KCNJ1, PTPRC, SLC25A12, SLC7A3, ATP1A1, ACSL1, SLC9A3, SLC9A2, CHP1, FXYD1, CPT1A, CPT1B, CCDC109B, NIPAL4, RHCG, SLC9A6, SLC26A2, TSC22D3, CCR1, MPC1, SLC22A5, CLCN1, SLC22A4 |
| GO:0009605 | Response to external stimulus | MR1, AFG3L2, RALB, CNGB1, TRPV4, FN1, RNF152, PKD1L2, CRY1, PRF1, LITAF, ATP1A1, STAT5B, FGF23, HLA-DRB1, ACSL1, LDLR, MAPT, ARG1, CD4, SLC38A3, ANG, BHLHE40, NGFR, STRC, INSR, RHCG, DNMT3A, DNMT3B, KCNJ2, IFITM2, DEPDC5, DMBT1, FOS, MAG, MST1R, HFE, RDH5, MRC1, VCAM1, CYP1A1, PDE4D, IFI44, KIT, RBM4B, HSPA8, SBNO2, DDX3X, SIK1, CD63, BAIAP2, IGHV3-23, USP2, NLRP1, MOG, SLC38A2, MUC5B, CRP, PROX1, ALOX5, XPR1, SLC25A25, MX1, IGLC6, ALPL, SIPA1, ASNS, PTPRC |
| GO:0098662 | Inorganic cation | PRKAG2, TRPV4, CNGB1, MICU1, ATP2A2, PKD1L2, NDUFA4, ATP1B1, SLC25A25, |

| | | |
|---|---|---|
| | transmembrane transport | TRPM2, SLC9B2, SLC4A4, KCNMA1, SLC12A3, ATP6AP1, KCNJ15, SLC30A3, SLC30A2, KCNJ2, SLC39A6, TRPM4, ATP6V1C1, TRPM5, SLC3A2, TRPV1, KCNJ1, ATP2B3, PTPRC, ATP1A1, SLC9A3, SLC9A2, CPT1A, CPT1B, CCDC109B, RHCG, SLC22A5, SLC9A6, SLC22A4 |
| GO:0098660 | Inorganic ion transmembrane transport | PRKAG2, TRPV4, CNGB1, ATP2A2, PKD1L2, NDUFA4, ATP1A1, ATP1B1, TRPM2, SLC9A3, GABRD, SLC9A2, SLC4A4, KCNMA1, SLC12A3, FXYD1, CLCN2, CPT1A, CPT1B, CCDC109B, ATP6AP1, KCNJ15, RHCG, SLC9A6, SLC22A5, KCNJ2, CLCN1, SLC3A2, SLC4A1, SLC26A2, SLC22A4, ATP2B3, MICU1, SLC25A25, SLC9B2, SLC30A3, SLC30A2, SLC39A6, TRPM4, ATP6V1C1, TRPM5, TRPV1, KCNJ1, PTPRC |
| GO:0015672 | Monovalent inorganic cation transport | PRKAG2, SLC38A3, CNGB1, ATP6AP1, SEC14L1, SLC5A7, SLC9A3R1, KCNJ15, WNK4, NDUFA4, KCNJ2, SLC44A4, ATP6V1C1, ATP1B1, TRPM5, SLC3A2, SLC38A4, KCNJ1, TRPM2, SLC9B2, SLC4A4, KCNMA1, SLC12A3, SLC38A2, ATP1A1, SLC9A3, SLC9A2, CHP1, CPT1A, CPT1B, RHCG, SLC9A6, SLC22A5, SLC22A4 |
| GO:0043269 | Regulation of ion transport | PLA2R1, SLC9A3R1, ATP1A1, NOS1AP, FGF23, CCR1, ATP1B1, FCRL5, AHCYL1, ARG1, SLC9A3, GSTO1, KCNMA1, CHP1, CD4, SLC38A3, FXYD1, CLCN2, KCNJ15, KCNJ2, GNAO1, CLCN1, SEPT5, CRHR1, HFE, TNFSF11, PDE4D, SIK1, WNK3, CD63, S100A1, DNM2, TRPM5, PLCB4, PER2, KCNJ1, GPER1 |
| GO:0048878 | Chemical homeostasis | TRPV4, GPR116, ALOXE3, PVALB, MICU1, FN1, SLC9A3R1, ATP2A2, XPR1, CRY1, WNK4, IRS1, ATP1B1, LDLR, UMOD, TRPM2, KCNMA1, NGFR, ATP6AP1, INSR, ADCY9, CCL14, CLDN4, SLC39A6, KCNJ2, ATP6V1C1, PTPN11, SLC4A1, TRPV1, HFE, SLC25A23, RAB38, GPER1, ATP2B3, PTPRC, ATP1A1, CCR1, FGF23, FLVCR1, SLC9A3, SLC9A2, SSTR5, KRT16, CHP1, CCDC109B, RHCG, SLC9A6, SOX4, SLC26A2, TNFSF11 |
| GO:1905039 | Carboxylic acid transmembrane transport | SLC38A3, PRKAG2, CPT1A, CPT1B, SLC22A4, SLC38A4, SLC6A6, SLC22A5, SLC25A12, SLC25A22, MPC1, SLC7A5, SLC25A15, SLC7A3, SLC38A2 |
| *Liver* | | |
| GO:0046949 | Fatty-acyl-CoA biosynthetic process | ACSL1, ACLY, ACSF2, ACACB, ELOVL6, TECR, ACLY, ELOVL5, ACSF2, ACACB, ELOVL6 |
| GO:0035337 | Fatty-acyl-CoA metabolic process | TECR, ACLY, DGAT1, ELOVL5, ACSF2, ACACB, ELOVL6, FAR1, ACSL1 |
| GO:0071616 | Acyl-CoA biosynthetic process | ACSL1, ACLY, ACSF2, ACACB, ELOVL6, TECR, ACSS2, ELOVL5 |
| GO:0035384 | Thioester biosynthetic process | TECR, ACLY, ELOVL5, ACSS2, ACSF2, ACACB, ELOVL6, ACSL1 |

| | | |
|---|---|---|
| GO:0032787 | Monocarboxylic acid metabolic process | ACSL1, C3, PDP1, FA2H, ACOX3, HK1, ACLY, UGT2B17, ACSF2, ACACB, ELOVL6, GCK, CYP7A1, CYP8B1, SC5D, ABCB11, TECR, GRHPR, UGT8, CYP2D6, UGT2B15, NR5A2, ABCD3, AACS, PKLR, ACSS2, ELOVL5, NPC1, P4HB, HPGD, PER2, OGDH, HOGA1, FADS6, MSMO1, CYP27A1 |
| GO:0008610 | Lipid biosynthetic process | ACSL1, ANG, FA2H, PHOSPHO1, ACLY, ST3GAL2, ACSF2, ACACB, ELOVL6, P2RX1, PPM1L, APOA4, PTDSS1, CYP7A1, SPTLC3, LSS, CYP8B1, SC5D, EBP, CYP3A4, ABCB11, DHCR24, TECR, UGT8, NPC1L1, MVK, ABCD3, CYB5R3, AGPAT4, FAR1, TM7SF2, HSD17B7, FDPS, ACSS2, FDFT1, ELOVL5, PMVK, MVD, C14orf1, PISD, SQLE, CYP51A1, FADS6, HMGCR, HMGCS1, DGAT1, NSDHL, MSMO1, IDI1, CYP27A1 |
| GO:0006631 | Fatty acid metabolic process | ACOX3, ACLY, ACSS2, ELOVL5, HPGD, SC5D, PER2, TECR, C3, FA2H, FADS6, CYP2D6, MSMO1, ACSF2, ABCD3, ACACB, ELOVL6, AACS, ACSL1 |
| GO:0006637 | Acyl-CoA metabolic process | ACSL1, ACLY, ACSF2, ACACB, ELOVL6, ELOVL5, ACSS2, PMVK, MVD, OGDH, TECR, PIPOX, DGAT1, MVK, FAR1 |
| GO:0035383 | Thioester metabolic process | ACLY, ELOVL5, ACSS2, PMVK, MVD, OGDH, TECR, PIPOX, DGAT1, MVK, ACSF2, ACACB, ELOVL6, FAR1, ACSL1 |
| GO:0035336 | Long-chain fatty-acyl-CoA metabolic process | ACSL1, ACLY, ACSF2, ELOVL6, TECR, DGAT1, ELOVL5, FAR1 |
| GO:0044255 | Cellular lipid metabolic process | SPTLC3, PGM3, PEX11A, ABCA1, PPM1L, APOA4, FA2H, UGT8, NPAS2, ACACB, ABCD3, AGPAT4, AACS, FAR1, P2RX1, ACLY, ELOVL5, HPGD, PMVK, PISD, PER2, SDC2, RDH11, DGAT1, SOAT1, ALAS1, IDI1, ELOVL6, CYP7A1, PTDSS1, ACOX3, KDELC2, SC5D, CYP3A4, TECR, CYP2D6, MVK, ANG, FDPS, FDFT1, ACSS2, MVD, C3, HMGCR, FADS6, HMGCS1, MSMO1, ACSF2, PDE3A, PHOSPHO1, ACSL1, ST3GAL2 |
| *Brain* | | |
| GO:0015074 | DNA integration | ERVK-11, GIN1, KRBA2, ERVK-10, NYNRIN |
| GO:0030198 | Extracellular matrix organization | ADAMTS3, ACTN1, COL22A1, FN1, SULF1, MMP13, FOXF2, PXDN, BCAN, SDC3, ELF3, LAMA5, ECM2, VCAN, NCAN, FBLN1, ACAN, ITGB8, DCN, NOXO1, COL12A1, FBN2, COL5A1 |
| GO:0043062 | Extracellular structure organization | BCAN, ITGB8, DCN, ELF3, NOXO1, COL12A1, VCAN, FBN2, ACAN, COL5A1, ADAMTS3, ACTN1, COL22A1, FN1, SULF1, MMP13, FOXF2, PXDN, SDC3, LAMA5, ECM2, NCAN, FBLN1 |
| **C. Cave upregulated** | | |
| *Gill* | | |
| GO:0006820 | Anion transport | PRKAG2, ATP8B4, CLCN2, CPT1A, CPT1B, SLC6A6, SLC9A3R1, SLC3A2, ACSL1, LDLR, |

| | | |
|---|---|---|
| | | SLC4A1, SLC4A4, SLC25A12, SLC25A22, SLC12A3, ATP8B1, SLC4A10, MTTP, SLC13A2, SLC7A8, ABCC2, SLC22A6, BAAT, FABP6, ABCB11, SLC6A13, APOA4, SLC12A1, TRPC4, CA4, CA2, SLC26A5, SLC26A3, SLC16A9, SLC34A2, CD36, P2RY6, SLC7A11, CA5B, PLA2G10, SLC1A3, SLC43A2, SLC25A1, SLC22A4, ABCA12, SLC26A11, CLCC1, VDAC1, SLC25A10, CFTR, AQP1 |
| GO:0055085 | Transmembrane transport | SLC4A10, SLC7A8, SLC9A1, COX5B, SLC14A2, ABCB11, SLC6A13, SLC12A1, TRPC4, COX15, COX11, SLC9A2, FTH1, ABCB1, KCNN3, SLC26A3, SLC16A9, SLC12A3, ATP6V1E1, GJA3, GJB2, SLC1A3, KCNK10, SLC39A1, SLC4A1, FKBP1B, SLC26A11, SLC2A4, CLCC1, VDAC1, CFTR, SLC5A1, AQP1, PRKAG2, SLC13A2, ABCC2, SLC22A6, SLC26A5, SCN4B, CYBRD1, SLC34A2, SLC7A11, SLC43A2, SLC25A1, SLC22A4, SLC31A1, ABCA12, FAM26D, HMOX2, SLC25A10, SLC28A1, CNGB1, MAL, SLC6A6, PRF1, NDUFA4, ATP1B1, SLC25A25, AHCYL1, TRPM2, SLC9A3, SLC9B2, SLC4A4, SLC25A22, CLCN2, CPT1A, CPT1B, ATP6AP1, SLC30A2, SLC9A6, CACNB2, SLC39A6, KCNJ2, SLC44A4, SLC3A2, TSC22D3, ATP2B3, SLC25A12, HSPA8, ATP8B1 |
| GO:0006811 | Ion transport | PRKAG2, ATP8B4, CNGB1, SLC6A6, SLC9A3R1, NDUFA4, ATP1B1, SLC25A25, ACSL1, LDLR, TRPM2, SLC9A3, SLC9B2, SLC4A4, SLC25A22, SLC12A3, CLCN2, CPT1A, CPT1B, ATP6AP1, SLC30A2, SLC9A6, CACNB2, SLC39A6, KCNJ2, SLC44A4, SLC3A2, SLC4A1, HFE, TSC22D3, ATP2B3, SLC25A12, ATP8B1, SLC4A10, MTTP, SLC7A8, SLC9A1, COX5B, SLC35G1, FABP6, ABCB11, SLC6A13, APOA4, SLC12A1, TRPC4, COX15, COX11, SLC9A2, FTH1, KCNN3, SLC26A3, SLC16A9, HEPHL1, ATP6V1E1, CD36, P2RY6, CA5B, PLA2G10, SLC1A3, KCNK10, SLC39A1, FKBP1B, SLC26A11, CLCC1, VDAC1, CFTR, SLC5A1, AQP1, COX17, SLC13A2, ABCC2, SLC22A6, BAAT, CA4, CA2, SLC26A5, LYN, SCN4B, SLC34A2, SLC7A11, UCP2, SLC43A2, SLC25A1, RAMP3, SLC22A4, SLC31A1, ABCA12, FAM26D, SLC25A10 |
| GO:0015711 | Organic anion transport | PRKAG2, SLC4A10, MTTP, SLC13A2, ABCC2, SLC7A8, SLC22A6, BAAT, FABP6, ABCB11, SLC6A13, APOA4, CA4, TRPC4, CA2, SLC26A5, SLC26A3, SLC16A9, SLC7A11, CD36, CA5B, PLA2G10, SLC1A3, SLC43A2, SLC25A1, SLC4A1, ABCA12, SLC22A4, SLC26A11, SLC25A10, CFTR, AQP1, ATP8B4, CPT1A, CPT1B, SLC6A6, SLC9A3R1, SLC3A2, ACSL1, LDLR, SLC4A4, SLC25A12, SLC25A22, ATP8B1 |
| *Liver* | | |
| N/A | N/A | N/A |
| *Brain* | | |
| N/A | N/A | N/A |
| **D. Cave downregulated** | | |

| *Gill* | | |
|---|---|---|
| GO:0006885 | Regulation of pH | MAFG, CA2, SLC26A5, SLC26A11, SLC26A3, CFTR, SLC26A2, ATP6AP1, SLC9A3, SLC9A2, RHCG, SLC9A6, CHP1 |
| GO:0006820 | Anion transport | PRKAG2, ATP8B4, CLCN2, CPT1A, CPT1B, SLC6A6, SLC9A3R1, SLC3A2, ACSL1, LDLR, SLC4A1, SLC4A4, SLC25A12, SLC25A22, SLC12A3, ATP8B1, ABCC2, CA5B, BAAT, SLC1A3, ABCB11, SLC6A13, CA4, TRPC4, SLC25A1, CA2, ABCA12, SLC26A5, SLC26A11, SLC26A3, CLIC2, SLC20A1, SLC25A10, CFTR, AQP1, SLC12A2 |
| GO:0015711 | Organic anion transport | PRKAG2, SLC38A3, ATP8B4, CPT1A, CPT1B, SLC6A6, SLC9A3R1, SLC22A5, SLC6A13, SLC3A2, ACSL1, LDLR, SLC26A2, SLC4A1, SLC22A4, SLC38A4, SLC4A4, SLC25A12, MPC1, SLC25A22, ATP8B1, ABCC2, CA5B, BAAT, SLC1A3, ABCB11, TRPC4, CA4, SLC25A1, CA2, ABCA12, SLC26A5, SLC26A11, SLC26A3, SLC25A10, CFTR, AQP1 |
| GO:0042592 | Homeostatic process | GSR, AKR1B1, ABCC2, SLC8A1, TRPC4, CA2, ARRDC3, PDK3, SLC26A5, FTH1, SLC26A3, GCLC, CYBRD1, GRIK2, PCK1, CXCR3, GATA2, UCP2, MUC6, MAFG, EPOR, SLC4A1, ABCA12, SLC26A11, PRDX1, FAM20A, CLDN1, SLC2A4, ALAS2, RAC1, NR1D2, CFTR, AQP1, NR1D1, TRPV4, CNGB1, ALOXE3, GPR116, FN1, SLC9A3R1, ATP2A2, CRY1, WNK4, IRS1, ATP1A1, STAT5B, FGF23, CCR1, ATP1B1, LDLR, FLVCR1, TRPM2, SLC9A3, SLC9A2, ATM, SSTR5, ITPKB, KCNMA1, KRT16, CHP1, MUC2, ANG, NGFR, CCDC109B, ATP6AP1, INSR, RHCG, SLC9A6, SOX4, CLDN4, SLC22A5, KCNJ2, SLC26A2, ERP44, HFE, TNFSF11, ATP2B3, PIGR |
| GO:0048878 | Chemical homeostasis | TRPV4, GPR116, ALOXE3, FN1, SLC9A3R1, ATP2A2, CRY1, WNK4, IRS1, ATP1A1, CCR1, FGF23, ATP1B1, LDLR, FLVCR1, SLC9A3, TRPM2, SLC9A2, SSTR5, KCNMA1, KRT16, CHP1, NGFR, CCDC109B, ATP6AP1, INSR, RHCG, SLC9A6, SOX4, CLDN4, KCNJ2, SLC4A1, SLC26A2, HFE, TNFSF11, ATP2B3, ABCC2, SLC8A1, TRPC4, CA2, PDK3, SLC26A5, SLC26A3, FTH1, CYBRD1, PCK1, GRIK2, CXCR3, GATA2, UCP2, MAFG, EPOR, ABCA12, FAM20A, SLC26A11, SLC2A4, CLDN1, ALAS2, NR1D2, CFTR, AQP1 |
| GO:0006811 | Ion transport | ABCC2, SLC8A1, BAAT, ABCB11, SLC6A13, TRPC4, CA4, CA2, SLC26A5, SLC2A6, FTH1, KCNN3, SLC26A3, CLIC2, SCN4B, SLC12A3, SLC12A2, HEPHL1, ADD2, GRIK2, CA5B, UCP2, SLC1A3, SLC25A1, SLC4A1, ABCA12, RAMP3, SLC26A11, FAM26D, CLDN10, SLC20A1, SLC25A10, CFTR, AQP1, AFG3L2, TRPV4, MAL, SLC6A6, ATP2A2, PRF1, NDUFA4, ATP1A1, ATP1B1, AHCYL1, SLC9A3, TRPM2, SLC9A2, SLC4A4, KCNMA1, FXYD1, CPT1A, CPT1B, CCDC109B, ATP6AP1, SLC5A7, NIPAL4, RHCG, SLC9A6, SLC44A4, SLC3A2, CYB561, SLC26A2, TSC22D3, ATP2B3, ABCB10, ATP8B1, PRKAG2, CNGB1, PKD1L2, FLVCR1, SLC38A4, GABRD, SLC25A22, MPC1, SLC38A3, CLCN2, |

| | | |
|---|---|---|
| | | KCNJ15, SLC22A5, KCNJ2, CLCN1, SLC22A4, SLC25A5, SLC25A12, HSPA8 |
| GO:0055085 | Transmembrane transport | ABCC2, SLC8A1, SLC14A2, ABCB11, SLC6A13, TRPC4, SLC26A5, SLC2A6, FTH1, KCNN3, SLC26A3, PPBP, CLIC2, SCN4B, SLC12A3, SLC12A2, CYBRD1, DMTN, ADD2, GRIK2, GJA3, GJB2, SLC1A3, SLC25A1, SLC4A1, ABCA12, SLC26A11, SLC2A4, FAM26D, SLC20A1, SLC25A10, CFTR, AQP1, AFG3L2, TRPV4, MAL, SLC6A6, ATP2A2, PRF1, NDUFA4, ATP1A1, ATP1B1, AHCYL1, SLC9A3, TRPM2, SLC9A2, SLC4A4, KCNMA1, FXYD1, CPT1A, CPT1B, CCDC109B, ATP6AP1, SLC5A7, NIPAL4, RHCG, SLC9A6, SLC44A4, SLC3A2, CYB561, SLC26A2, TSC22D3, ATP2B3, ABCB10, ATP8B1, PRKAG2, CNGB1, PKD1L2, FLVCR1, SLC38A4, GABRD, SLC25A22, MPC1, SLC38A3, CLCN2, KCNJ15, SLC22A5, KCNJ2, CLCN1, SLC22A4, SLC25A5, SLC25A12, HSPA8 |
| GO:0098656 | Anion transmembrane transport | SLC4A1, SLC26A5, SLC26A11, SLC26A3, CLIC2, SLC20A1, CFTR, SLC1A3, SLC12A3, SLC12A2, SLC38A3, FXYD1, PRKAG2, CLCN2, CPT1A, CPT1B, SLC6A6, SLC22A5, CLCN1, SLC26A2, SLC38A4, SLC22A4, GABRD, SLC4A4, SLC25A12, MPC1, SLC25A22 |
| GO:0055067 | Monovalent inorganic cation homeostasis | SLC26A2, ATP6AP1, SLC9A3, SLC9A2, RHCG, SLC9A6, ATP1A1, KCNJ2, KCNMA1, CHP1, ATP1B1, MAFG, CA2, SLC26A5, SLC26A11, SLC26A3, SLC8A1, CFTR |
| *Liver* | | |
| GO:0042221 | Response to chemical | IL18, IL12B, LGALS1, TRIM25, NCOA3, MMP2, CCL16, CYCS, P2RY1, CD38, P2RX7, EIF4EBP1, SCARB1, CCL14, CLDN4, PTGR1, IL1R1, IL1B, TRIM16, GUCY2C, LMO2, CCL21, IL6R, PDE1B, GLUL, PLK3, TNC, ARSB, SLC12A5, SPHK1, PDGFRA, ACVR1, PDGFB, CA2, MX1, PTGS1, PTGS2, PPBP, FZD4, ADCY1, LRP8, ADD3, S100P, GNB3, CDKN1A, C3, GNAI2, IRF3, HID1, SIDT2, PDE4B, S100A16, IFIT1, SLC9A1, SLC8A1, CDK19, ERO1L, CHKA, KDM6B, NFKBIA, CHAT, LIPG, NLRP1, HGF, DSG2, NPNT, TESC, VCAM1, MSN, BAX, STAT1, ERN1, CYP26B1, UBB, CORO1B, IKBKE, JAK2, CD9, PLA2G1B, GRN, SSTR5, CLU, EIF2AK2, CD4, EPHA3, BDKRB2, SERPINH1, TNFRSF14, IGF1, RIPK2, TRIM21, CBX3, UCP2, TGFBR2, CXCL2, YES1, NLRP12, ACAP2, MB21D1, FAM162A, ERBB2, ABCG5, FLT3, PAQR9, ABCA1, CD274, APOA4, MTHFR, AGL, ABCD3, PPP5C, GCH1, GCK, AACS, P2RX1, ACO1, P4HB, ADNP2, EZR, PMVK, AHR, CCL3, CRHR1, CALU, CYB5A, SDC2, APRT, VCP, CYP7A1, H2AFZ, EEF2K, CRY1, NTRK3, DHCR24, NFIL3, NPC1L1, FZD7, NDRG1, BCAR3, BRSK2, SERPINF1, PKLR, ITPR2, ANG, CDK4, S100B, RORB, NPC1, SORT1, EPB41L5, COL4A2, SQLE, HMGCR, HMGCS1, MLXIPL, CCRN4L, PRKCA, SREBF2, SETD7, STT3B, PDE3A |
| GO:0010033 | Response to organic substance | FLT3, PAQR9, ABCA1, CD274, APOA4, MTHFR, AGL, GCH1, PPP5C, ABCD3, AACS, GCK, TRIM25, P2RX1, CCL14, ADNP2, EZR, PMVK, AHR, CCL3, CRHR1, CALU, SDC2, |

| | | |
|---|---|---|
| | | APRT, VCP, CYP7A1, H2AFZ, EEF2K, CRY1, NTRK3, DHCR24, NFIL3, FZD7, SERPINF1, BRSK2, PKLR, ITPR2, ANG, CDK4, S100B, RORB, NPC1, SORT1, EPB41L5, COL4A2, C3, SQLE, HMGCR, HMGCS1, MLXIPL, CCRN4L, PRKCA, SREBF2, SETD7, STT3B, PDE3A, IFIT1, IL18, SLC9A1, SLC8A1, CDK19, IL12B, LGALS1, CHKA, NCOA3, MMP2, CCL16, P2RY1, P2RX7, CD38, EIF4EBP1, SCARB1, NFKBIA, CHAT, CLDN4, IL1R1, IL1B, NLRP1, HGF, DSG2, TRIM16, NPNT, TESC, VCAM1, LMO2, CCL21, MSN, IL6R, BAX, PDE1B, GLUL, STAT1, TNC, ARSB, SPHK1, ERN1, CYP26B1, ACVR1, PDGFB, CORO1B, IKBKE, CA2, JAK2, MX1, CD9, PLA2G1B, GRN, PTGS1, SSTR5, CLU, PTGS2, FZD4, PPBP, EIF2AK2, LRP8, ADCY1, CD4, EPHA3, S100P, GNB3, SERPINH1, IGF1, TNFRSF14, RIPK2, TRIM21, CBX3, CDKN1A, UCP2, TGFBR2, IRF3, HID1, CXCL2, YES1, ACAP2, NLRP12, MB21D1, SIDT2, ERBB2, PDE4B |
| GO:0014070 | Response to organic cyclic compound | BAX, IFIT1, IL18, STAT1, SLC9A1, TNC, ARSB, SLC8A1, SPHK1, ACVR1, PDGFB, CA2, PTGS1, LGALS1, GRN, PTGS2, SSTR5, CHKA, EIF2AK2, ADCY1, LRP8, TRIM25, CD4, NCOA3, P2RY1, CD38, P2RX7, IGF1, NFKBIA, RIPK2, CLDN4, CDKN1A, CBX3, IL1B, TGFBR2, IRF3, C3, HID1, MB21D1, DSG2, VCAM1, MSN, PDE4B, CYP7A1, H2AFZ, EEF2K, FLT3, PAQR9, ABCA1, NTRK3, APOA4, MTHFR, AGL, ABCD3, SERPINF1, PPP5C, AACS, PKLR, P2RX1, ITPR2, CDK4, S100B, NPC1, EZR, PMVK, AHR, CCL3, CALU, SDC2, HMGCS1, PDE3A |
| GO:0065008 | Regulation of biological quality | SLC4A10, EXOSC9, NCOA5, ACE, LGALS1, P2RY1, CD38, P2RX7, TENM1, SCARB1, HPS5, CCL14, BLK, CLEC4M, CLDN4, IL1R1, IL1B, STEAP4, CCL21, PDE1B, C9, GLUL, IL20RA, CDHR5, RHOU, LPCAT1, GLRX, SPHK1, SLC12A5, CYP3A4, PDGFRA, PDGFB, GZMB, CA2, RASSF2, USH1C, ITGAV, PTGS1, PTGS2, PPBP, FZD4, ADCY1, LRP8, ITGB3, PALM2, GNB3, CRTC1, C3, SWAP70, GNAI2, PTPN6, L1CAM, ITGA6, SIDT2, PDE4B, FHOD3, ALOXE3, F8, SLC9A1, SLC8A1, SFXN5, CAMK2G, ATP1B3, SLC6A13, ERO1L, AGTRAP, AGTR1, PNPLA2, TSPAN8, SLC1A1, HK1, GAA, CXCR3, NFKBIA, CHAT, EPB41L3, LIPG, HGF, NCF1, SLC4A1, RDH11, DSG2, CYSLTR1, TESC, MSN, CYBB, BAX, CRP, STAT1, ERN1, CCR1, CYP26B1, UBB, CORO1B, ATP8A1, JAK2, GNA13, CD9, PLA2G1B, CLU, SSTR5, CD2, CLIC2, EIF2AK2, ITPR1, TFPI, CD4, ANGPT1, BDKRB2, SERPINE2, RBFOX2, IGF1, TRIM21, TGM2, HCAR2, ANO9, UCP2, YES1, DOC2B, NLRP12, PLEKHO1, NR1D2, PIGR, SYT12, SMDT1, QRSL1, SEPT7, A2M, ABCG5, FLT3, PEX11A, ABCA1, SUN3, APOA4, HLA-DRB1, MTHFD1, TMEM97, FLNB, ZFP36L2, NR5A2, ACACB, GCH1, AACS, HPX, GCK, P2RX1, MYO10, XCR1, HSD17B7, ACO1, P4HB, EZR, LEPRE1, RAB20, SULT1A1, PYGL, CCL3, PER2, KCNK6, CRHR1, CALU, HEBP2, DGAT1, CREBL2, RAB11FIP5, ACTG1, SOAT1, APRT, DISC1, VCP, |

| | | |
|---|---|---|
| | | MYO5B, CLOCK, ARNTL, CYP7A1, LSS, ACOX3, GLUD1, MCU, ITGAM, DNAJC5, CRY1, SIPA1L1, NTRK3, IGSF9B, CNNM2, PPP1R3G, ISCU, ITGAX, BRSK2, SERPINF1, ITPR2, SULT1B1, ANG, CDK4, S100B, NPC1, HPSE, HMGCR, SPTBN1, MLXIPL, CCRN4L, PRKCA, SREBF2, PDE3A, EPS8 |
| GO:0050708 | Regulation of protein secretion | ARNTL, ANG, MCU, GLUD1, CRP, EZR, LEPRE1, CD274, CCL3, PER2, HLA-DRB1, SPTBN1, HMGCR, RAB11FIP5, PRKCA, BRSK2, GCK, CLOCK, AACS, BTN2A2, ITPR2, ANGPT1, RSAD2, GLUL, CD38, P2RX7, CLEC4E, IGF1, TNFRSF14, BLK, HCAR2, IL1B, UCP2, NLRP1, IRF3, DOC2B, NLRP12, TRIM16, JAK2, PLA2G1B, SSTR5, CD2, ITPR1, SIDT2 |
| *Brain* | | |
| N/A | N/A | N/A |

# Supplementary figures

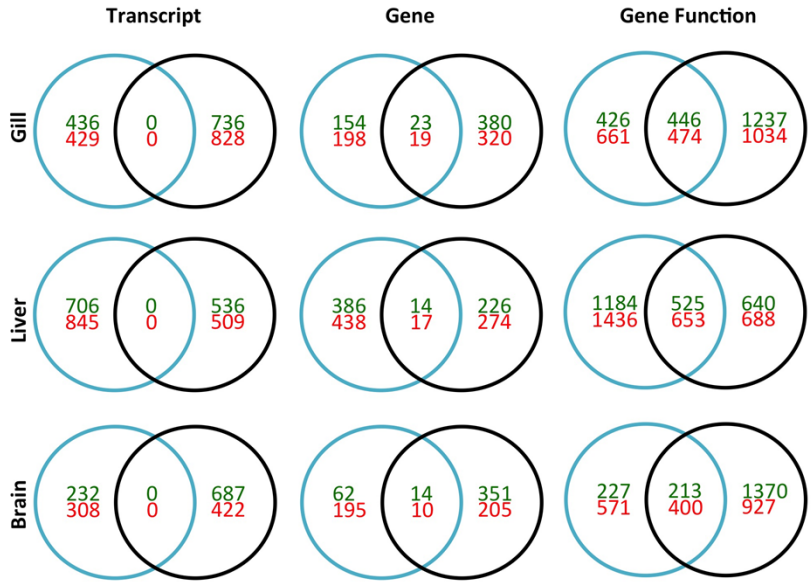


**Figure S1:** Venn diagrams depicting the number of unique and shared expression responses in the two cave habitats at the level of transcripts, genes, and functional annotation. These numbers were the basis for the calculation of the Jaccard index used to analyze shared responses among habitats, organs, and levels of biological organization. Light blue circles are the nonsulfidic cave and black circles are the sulfidic cave population.

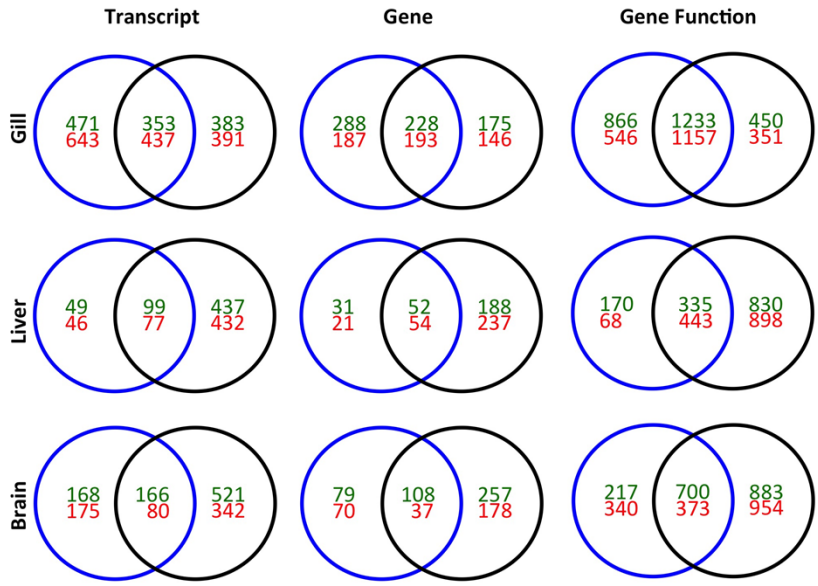


**Figure S2:** Venn diagrams depicting the number of unique and shared expression responses in the two sulfidic habitats at the level of transcripts, genes, and functional annotation. These numbers were the basis for the calculation of the Jaccard index used to analyze shared responses among habitats, organs, and levels of biological organization. Dark blue circles are the sulfidic surface and black circles are the sulfidic cave population.

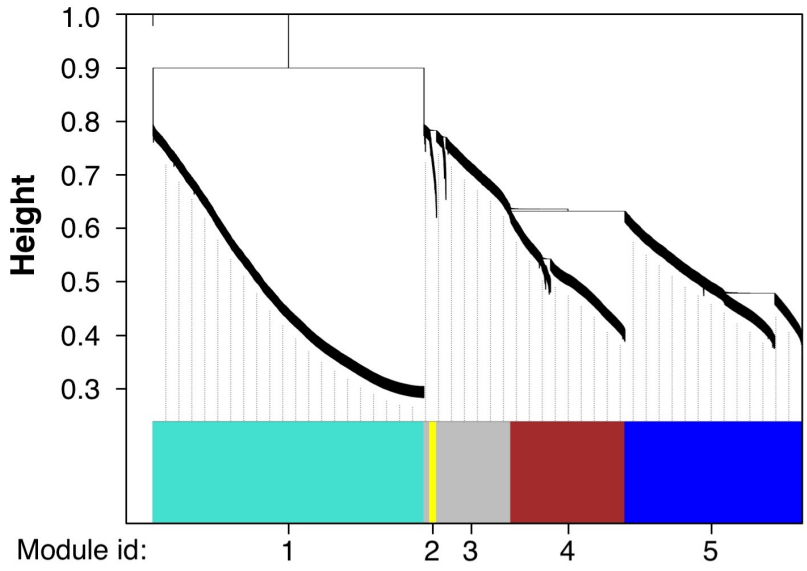


**Figure S3** Results of the weighted co-expression network analysis. The linkage clustering dendrogram depicts modules of co-expressed genes (numbered color bars below). Correlation between module eigenvalues and predictor variables can be found in Table 1 of the main manuscript.

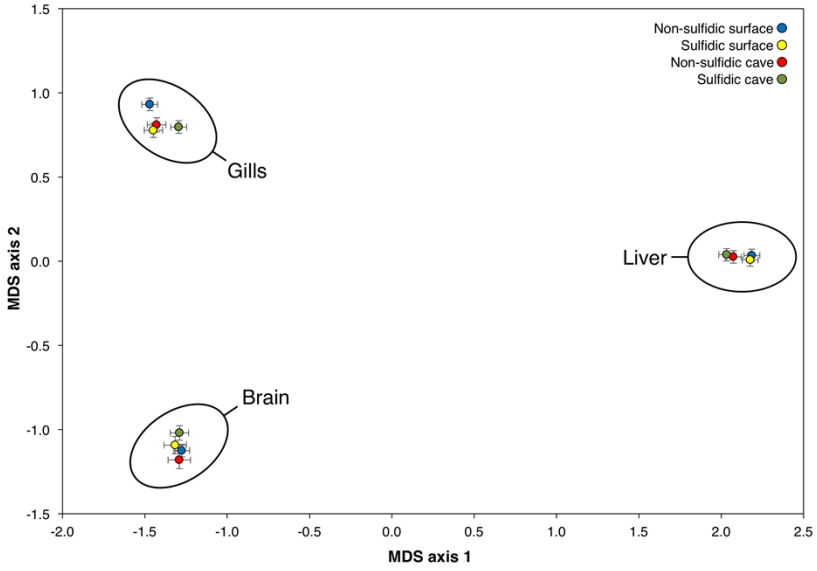


**Figure S4:** MDS plot of the top 10,000 expressed genes indicates pronounced differences in expression profiles among the three organs analyzed in this study. Depicted are means (± standard error) for each organ and population (color coded as in legend).

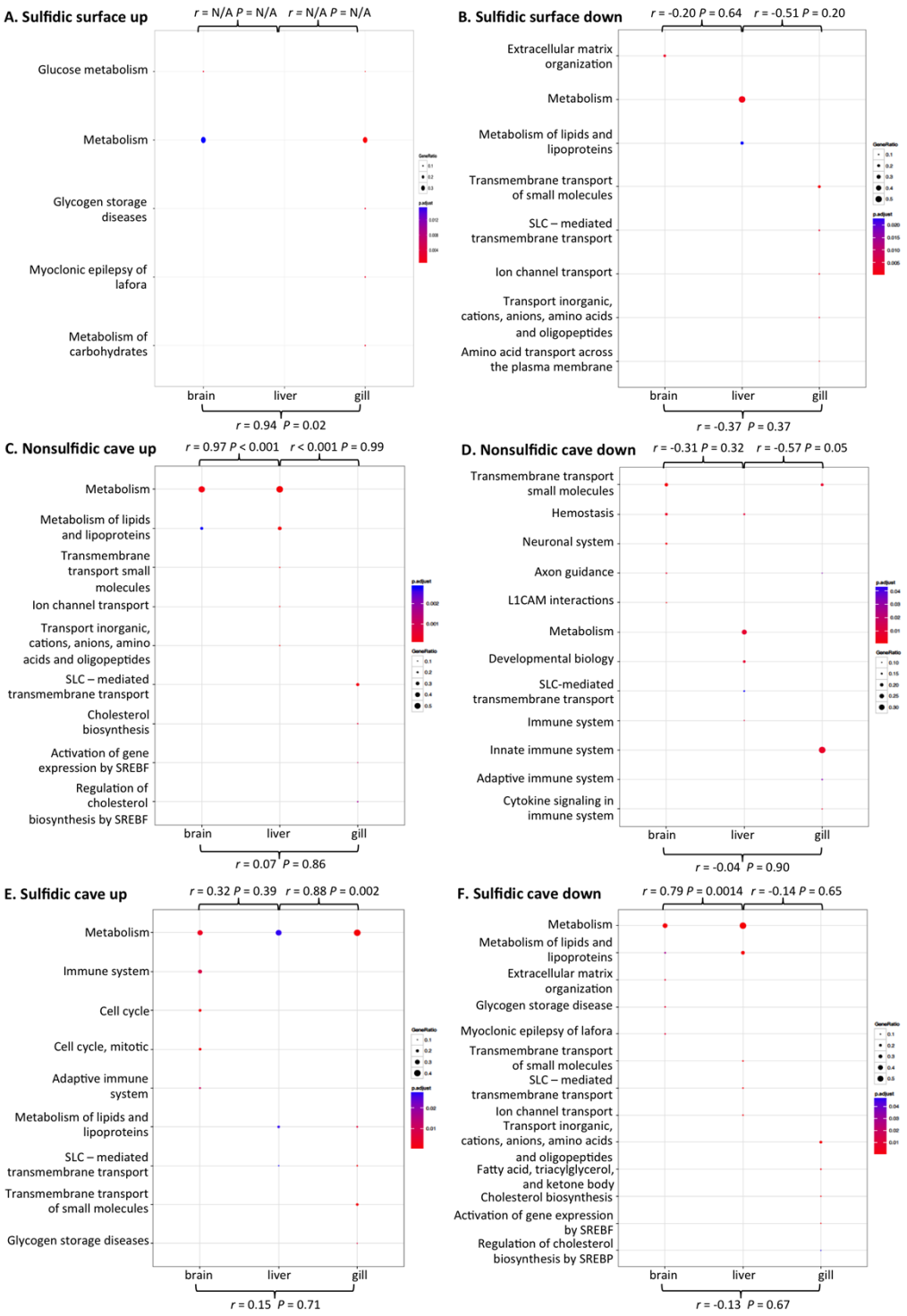


**Figure S5**: Comparison of the functional annotations of up and downregulated genes among organs. Depicted are the enriched reactome pathways of for each of the three extremophile populations: (A-B) sulfidic surface, (C-D) nonsulfidic cave, (E-F) sulfidic cave. The size of each dot corresponds to the number of genes in enriched each pathway (i.e., gene ratio). The color corresponds to the adjusted *P*-value for each category as indicated by the scale bar. Pearson correlation coefficients (*r*) and *P*-values indicate similarities in enrichment among organs.

# Supplementary analyses: evolutionary relationships among focal populations

The number of shared differentially expressed genes at each level of organization may be a function of phylogenetic relatedness, as the shared responses may be higher in the sulfidic populations due to them being more closely related (Tobler *et al.* 2008). To address this, we analyzed SNPs in our RNA-seq data to assess the evolutionary relationships among focal populations. To increase sample size, we also included additional populations from the same and different river drainages (Palacios *et al.* 2013) based on the availability of previously published data (Kelley *et al.* 2016).

## *Methods*

*SNP calling*

After read mapping, bam files from the same individual were combined into single bam file using the MergeSamFiles command in Picard Tools (v 1.138) (http://broadinstitute.github.io/picard/). In addition to data collected for this study, we also included sequences from Kelley *et al.* (2016) in the analysis to gain a comprehensive view on relationship patterns *Poecilia* populations in the region. The additional data included two pairs of sulfidic and non-sulfidic populations from additional drainages (Pichucalco and Puyacatengo; Tobler *et al.* 2008), and additional site in the Cueva del Azufre system (El Azufre I), and additional samples for the nonsulfidic surface population in the Tacotalpa river drainage (Arroyo Bonita).

Single nucleotide polymorphisms (SNP) were called on a per population basis using the UnifiedGenotyper tool in the Genome Analysis Toolkit (GATK) with EMIT ALL SITES (v. 3.5; McKenna et al., 2010). Population vcf files were merged using the CombineVariants tool in GATK. The combined vcf was filtered following GATK recommended best practices (DePristo *et al.* 2011; Van der Auwera *et al.* 2013). The GATK-filtered vcf was subsequently filtered using vcftools (v. 0.1.12b; Danecek *et al.* 2011) to include only biallelic sites that had at least 8-fold coverage per individual in 90% of the individuals. We also filtered the vcf such that no sites were within 5000 base pairs of one another. We excluded singletons for analyses that are sensitive to singletons (i.e., ADMIXTURE; Alexander *et al.* 2009).

*Population structure and relatedness analyses*

We tested for evidence for population structure using the program ADMIXTURE (v. 1.23; Alexander *et al.* 2009). Vcf files (which included all populations) were converted into ped format using vcftools. We performed ten different runs for each independent value of K from 1-12 to test for convergence. We selected the best-supported K according to the cross-validation protocol implemented in ADMIXTURE.

To investigate population relatedness, we implemented TreeMix (v. 1.12; Pickrell & Pritchard 2012), which assembles a maximum likelihood bifurcating tree of population relatedness. Ped files were converted to TreeMix format using a python script that was included with the distribution of TreeMix. We rooted the tree using the sulfidic population from the Rio Pichucalco drainage lineage (*Poecilia sulphuraria*; Pfenninger *et al.* 2014). The percentage of variance explained increased when we allowed one migration event (-m 1) (from 98.9% to 99.4%).

## *Results*

A total of 7616 SNPs passed our filters for the ADMIXTURE analysis, and 8368 SNPs passed our filters for the TreeMix analysis. In the ADMIXTURE analysis, the best-supported model for population structure was K = 4 (Fig. S6). Puyacatengo sulfidic and non-sulfidic populations

clustered together as one population, as did the extremophile populations (sulfidic surface, nonsulfidic cave and sulfidic cave) in the Tacotalpa. The Pichucalco sulfidic population was recovered as an independent cluster, whereas the Pichucalco nonsulfidic population clustered with the non-sulfidic population from Tacotalpa.

In the bifurcating tree generated using TreeMix (Fig. S7), the two cave populations from the Tacotalpa form a monophyletic group that is nested within the two sulfidic populations (El Azufre I and II). The non-sulfidic Tacotalpa population is most closely related to the four extremophile populations in the same drainage. Puyacatengo populations (sulfidic and nonsulfidic) were most closely related to one another. Without migration, the tree explains 98.9% of the variance in the dataset and exhibits the same topology. One migration event from the Pichucalco non-sulfidic population to the Tacotalpa non-sulfidic population was supported and explained 99.4% of the variance.

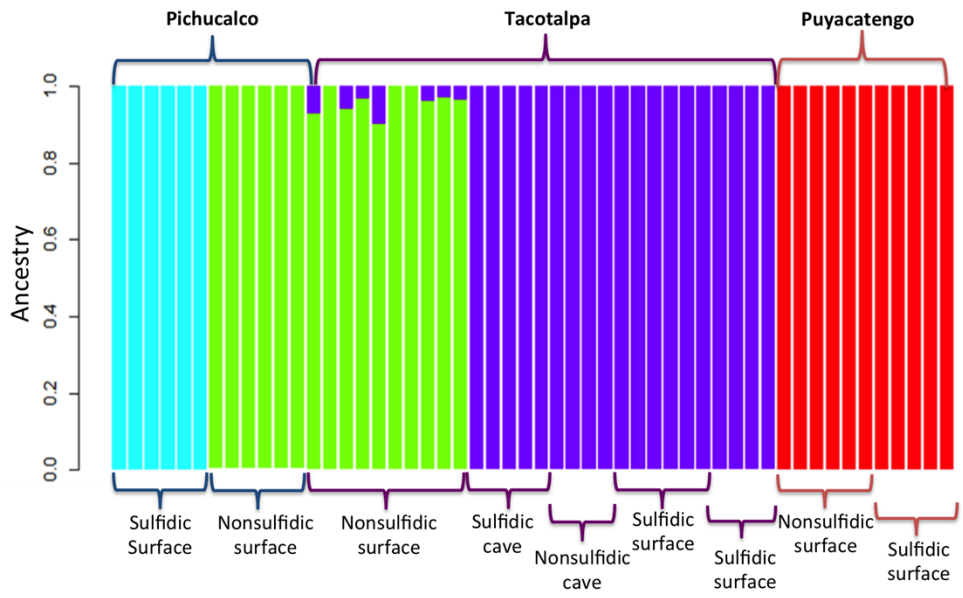


**Figure S6:** Output from the program ADMIXTURE based on the best-supported model (K = 4). Note that the focal extremophile populations in the Tacotalpa represent a single cluster (purple) without significant population structure. Drainage of origin is noted as the top of the plot.

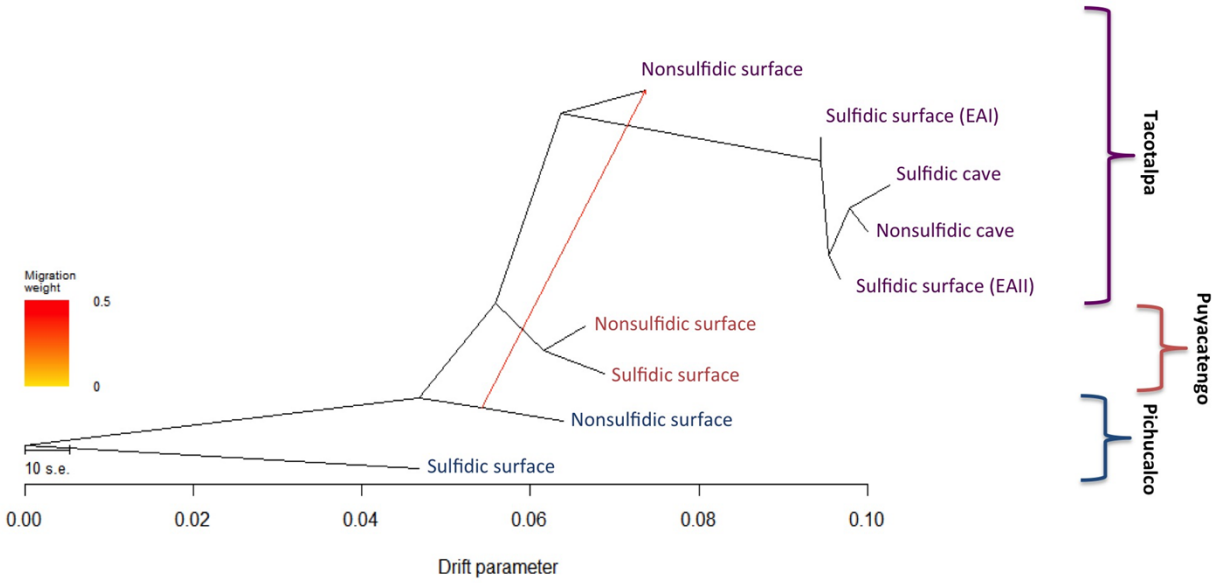


**Figure S7:** Treemix plot of the best model that includes one migration event from the nonsulfidic surface in the Pichucalco drainage, to the nonsulfidic surface in the Tacotalpa drainage. Populations in the Pichucalco drainage are designated in blue, populations in the Tacotalpa are designated in purple and populations in the Puyacatengo are designated in red.

## Supplementary references


Alexander DH, Novembre J, Lange K (2009) Fast model-based estimation of ancestry in unrelated individuals. *Genome Research* **19**, 1655-1664.

Danecek P, Auton A, Abecasis G*, et al.* (2011) The variant call format and VCFtools. *Bioinformatics* **27**, 2156-2158.

DePristo MA, Banks E, Poplin R*, et al.* (2011) A framework for variation discovery and genotyping using next-generation DNA sequencing data. *Nature Genetics* **43**, 491-498.

Kelley JL, Arias-Rodriguez L, Martin DP*, et al.* (2016) Mechanisms underlying adaptation to life in hydrogen sulfide–rich environments. *Molecular Biology and Evolution* **33**, 1419-1434.

McKenna A, Hanna M, Banks E*, et al.* (2010) The Genome Analysis Toolkit: a MapReduce framework for analyzing next-generation DNA sequencing data. *Genome Research* **20**, 1297-1303.

Palacios M, Arias-Rodriguez L, Plath M*, et al.* (2013) The rediscovery of a long described species reveals additional complexity in speciation patterns of poeciliid fishes in sulfide springs. *PLoS One* **8**, e71069.

Pfenninger M, Lerp H, Tobler M*, et al.* (2014) Parallel evolution of cox genes in H2S-tolerant fish as key adaptation to a toxic environment. *Nature Communications* **5**, 3873.

Picardtools: http://broadinstitute.github.io/picard/

Pickrell JK, Pritchard JK (2012) Inference of population splits and mixtures from genome-wide allele frequency data. *PLoS Genetics* **8**, e1002967.

Tobler M, Dewitt TJ, Schlupp I*, et al.* (2008) Toxic hydrogen sulfide and dark caves: phenotypic and genetic divergence across two abiotic environmental gradients in *Poecilia mexicana*. *Evolution* **62**, 2643-2659.

Van der Auwera GA, Carneiro MO, Hartl C*, et al.* (2013) From FastQ data to high confidence variant calls: the Genome Analysis Toolkit best practices pipeline. *Curr Protoc Bioinformatics* **43**, 11 10 11-33.